Animal Diseases

Open Access

Lactobacillus plantarum A3 attenuates ulcerative colitis by modulating gut microbiota and metabolism

Songkang Qin[1], Yingli Wang[1], Mengjie Yang[1], Pengpeng Wang[1], Mudassar Iqbal[1,2], Jinquan Li[1,3,4] and Yaoqin Shen[1*]

Abstract

Antibiotics are widely used to treat various diseases. However, growing evidence indicates that antibiotic therapy in human life increases the incidence of inflammatory bowel disease (IBD). Therefore, we need appropriate methods to reduce the incidence or symptoms of IBD. In this study, we used lincomycin hydrochloride to construct a gut microbial dysbiosis model in mice, and then, constructed an ulcerative colitis (UC) model. Meanwhile, we used *Lactobacillus plantarum* A3 from equine to treat UC in mice with gut microbial dysbiosis. The results showed that lincomycin hydrochloride had little effect on the small gut microbiota in mice, but had a more destructive effect on the large intestin. *Lactobacillus plantarum* A3 alleviated the symptoms of UC in mice, which was reflected in its significantly reduced spleen index and disease activity index (DAI) ($p < 0.05$), inhibited the shortening of colon and alleviated the invasion of inflammatory cells in the colon. Moreover, we found that it played a mitigatory role by inhibiting oxidative stress and regulating inflammatory cytokines in mice. At the same time, it restored the diversity and composition of the colonic microbiota and significantly increased the abundance of beneficial bacteria such as *Blautia* and *Akkermansia* ($p < 0.05$); Notably, it significantly increased the concentrations of arachidonoyl ethanolamide phosphate (AEA-P) and cortisone ($p < 0.05$) which have analgesic and anti-inflammatory effects. In conclusion, our study found that *Lactobacillus plantarum* A3 has the potential to regulate UC in mice with gut microbial dysbiosis.

Keywords Antibiotics, Gut microbiota, *Lactobacillus plantarum*, DSS, Ulcerative colitis, Untargeted metabolomics

Introduction

Inflammatory bowel disease (IBD) is a nonspecific chronic intestinal inflammatory disease, that includes ulcerative colitis (UC) and Crohn's disease (CD). UC mainly occurs in the colon and rectum, and spreads to the cecum as the disease progresses, while CD can occur anywhere in the intestine, generally from superficial ulcers to deep spread (Imhann et al. 2018). On the one hand, IBD is difficult to cure, prone to recurrent attacks and has a risk of carcinogenesis at a later stage; on the other hand, IBD has gradually become a disease with an increasing incidence in modern society. Not only are there more cases in developed countries such as Europe and the United States, but the incidence is also increasing in regions with faster

*Correspondence:
Yaoqin Shen
yshen@mail.hzau.edu.cn
[1] College of Veterinary Medicine, Huazhong Agricultural University, Wuhan 430070, People's Republic of China
[2] Faculty of Veterinary and Animal Sciences, The Islamia University of Bahawalpur, Bahawalpur 63100, Pakistan
[3] Key Laboratory of Environment Correlative Dietology, Interdisciplinary Sciences Institute, College of Food Science and Technology, Huazhong Agricultural University, Wuhan, China
[4] State Key Laboratory of Agricultural Microbiology, Huazhong Agricultural University, Wuhan, China

Qin *et al. Animal Diseases*   (2023) 3:16

Page 2 of 18

economic development such as Asia, Africa and South America (Glassner et al. 2020). Therefore, IBD has gained increasing attention. Unfortunately, the real cause of IBD has not been explored.

Recently, it has been demonstrated that antibiotics may be one of the causes of IBD. A study involving 107,2426 research projects and nearly 660,000 follow-up results revealed that the incidence of IBD in children who were unexposed and exposed to antibiotic treatment was 0.83‰ and 1.52‰, respectively, indicating that children exposed to antibiotic treatment had an 84% increased risk of IBD in later stages. In addtiton, it has been proven that the occurrence of IBD is negatively correlated with age (Kronman et al. 2012). Consistent with studies in children, adults exposed to antibiotic therapy also have an increased risk of IBD. An investigation covering 23,982 IBD patients (15,951 with UC, 7898 with CD, and 133 with unnamed IBD) spanning 10 years indicated that patients who used antibiotics for more than 1 year had 88, 74, and 127% increased risk of IBD, UC and CD compared with patients who did not use antibiotics ($p < 0.001$) (Nguyen et al. 2020). In addition, after mice were intervened by antibiotics, their gut microbiota was changed, and their sensitivity to dextran sulfate sodium (DSS) was increased, which means that they were more likely to induce UC (Ozkul et al. 2020). Therefore, based on gut microbial dysbiosis, it is very important to use appropriate drugs and preparations to restore gut microbiota, and reduce the incidence or symptoms of IBD.

Studies have shown that probiotics can not only alter the expression of inflammatory cytokines in the body and reduce the severity of inflammation (Yu et al. 2020), but also change the gut microbiota such as the number, activity, and microbiota composition (Ma et al. 2020; Li et al. 2021a, 2021b, 2021c). Currently, probiotics have been used as IBD therapy to modulate the gut microbiota of the host (Biagioli et al. 2020; Oka and Sartor 2020). This suggests that probiotics may reduce the incidence of IBD or alleviate symptoms of IBD when used in IBD patients with gut microbial dysbiosis. *Lactobacillus plantarum* A3 is a probiotic with good properties that has been isolated and screened in healthy adult horses, and has a significant recovery effect on DSS-induced UC in mice (Qin et al. 2022). Therefore, the aim of this study was to investigate the regulatory effect of *Lactobacillus plantarum* A3 from equine on UC in mice with gut microbial dysbiosis and provide a reference for subsequent screening of potential mitigatory agents.

Results

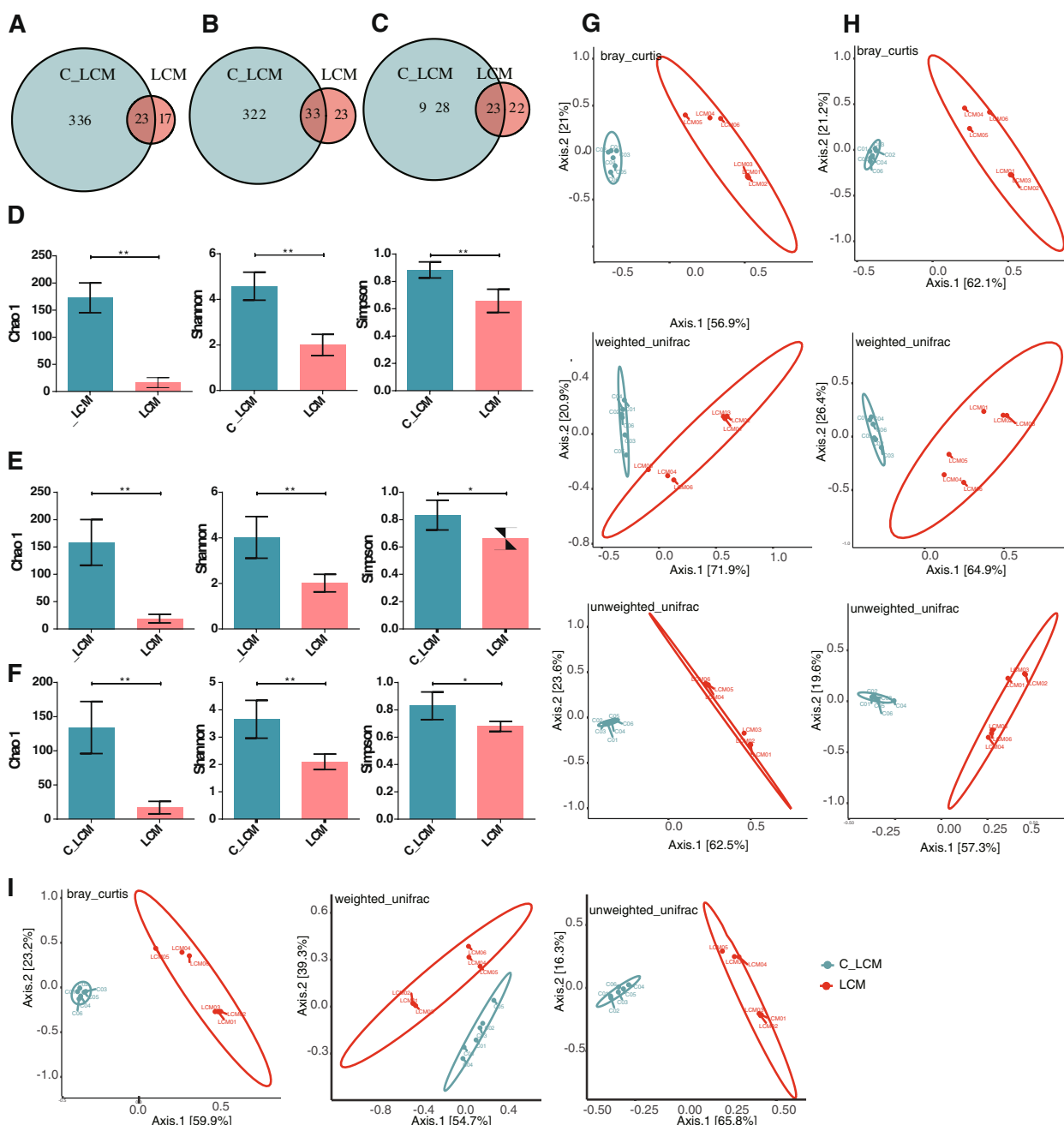### Lincomycin had a more destructive effect on the large gut microbiota in mice

To establish a mouse model of gut microbial dysbiosis, we treated the mice with lincomycin hydrochloride and analyzed the changes in gut microbiota in the duodenum, jejunum, ileum, cecum, colon and rectum. Compared with the C_LCM group, the number of OTUs in the duodenum, jejunum and ileum did not change much, and even the number of OTUs in the duodenum increased (Fig. S1 A-C). However, the rectum decreased significantly after exposure to lincomycin hydrochloride in the LCM group ($p < 0.01$) (Fig. 1A-C). Regarding the alpha diversity, there was no significant change in Chao 1, Shannon and Simpson indexes of duodenum, jejunum and ileum in the LCM group, cecal, colonic and rectal microbiota were significantly decreased ($p < 0.05$) (Fig. 1D-F, Fig. S1 d-f). These results indicated that lincomycin hydrochloride had a greater effect on the number and diversity of microbiota in the large intestine of mice than in the small intestine of mice.

Based on the results of OTUs and alpha diversity analysis, we focused our analysis on beta diversity of cecal, colonic and rectal microbiota in mice. PCoA and ANO-SIM analysis were performed by calculating Bray-Curtis, weighted UniFrac and unweighted UniFrac distances. The results showed that there were significant differences in beta diversity between the LCM group and the C_LCM group ($p < 0.01$) (Fig. 1G-I, Table S3), which indicated that lincomycin hydrochloride significantly altered the microbiota structure of the mouse cecum, colon and rectum. The above results showed that lincomycin hydrochloride had little effect on the microbiota of the small intestine (duodenum, jejunum and ileum), but had more destructive effect on the large intestine (cecum, colon and rectum) after intervention in mice.

Lactobacillus plantarum A3 can alleviate the symptoms of ulcerative colitis in mice

To further study the effect of equine *Lactobacillus plantarum* A3 on ulcerative colitis in mice with gut microbial dysbiosis, clinical indexes of mice were analyzed (Fig. 2A). During the 7-day period of DSS intervention, body weight changes and DAI index of mice in each group were monitored, and the results showed that except for the control group, which showed a stable and slow upward trend, the body weight of mice in the other three groups showed a downward trend with DSS intervention, and more obvious over time, and eventually, body weight decreased to the lowest level on the last day (Fig. 2B). In addition, except for the control group, the DAI index of mice tended to be stable, and the DAI index of mice in the other three groups showed upward trend over time. Notably, the increasing trend of DAI in the DSS group was the fastest, and at the end of the experiment, the DAI index in the DSS group was significantly higher than that in other groups ($p < 0.05$) (Fig. 2C, D). These results also showed that both *Lactobacillus*

Qin *et al. Animal Diseases*   (2023) 3:16

Page 3 of 18

Fig. 1 Lincomycin had a more destructive effect on the large gut microbiota in mice. **A–C** Venn diagram (**A**: Cecum; **B**: Colon; **C**: Rectum); **D-F** Alpha diversity (**D**: Cecum; **E**: Colon; **F**: Rectum); $^{ns}p > 0.05$, $*p < 0.05$, $**p < 0.01$; **G-I** Based on PCoA, beta diversity of different intestinal segment contents in mice (**G**: Cecum; **H**: Colon; **I**: Rectum)

plantarum A3 and butyrate slowed the increasing trend of the DAI index. After the experiment, the mice were euthanized and dissected. The results showed that compared with the control group, the spleen index of mice in the DSS group was significantly increased ($p < 0.05$) (Fig. 2E), but the colon length was significantly shorter ($p < 0.05$) (Fig. 2F). The spleen index and colon length of

mice in the LP_DSS group were similar to the control group. This showed that *Lactobacillus plantarum* A3 can prevent the occurrence of UC, and more evidence appeared in the longer colon length and lighter color of colonic contents in the LP_DSS group (Fig. 2F).

After mouse colon tissue was stained by H&E, the colonic injury were further observed. Compared with
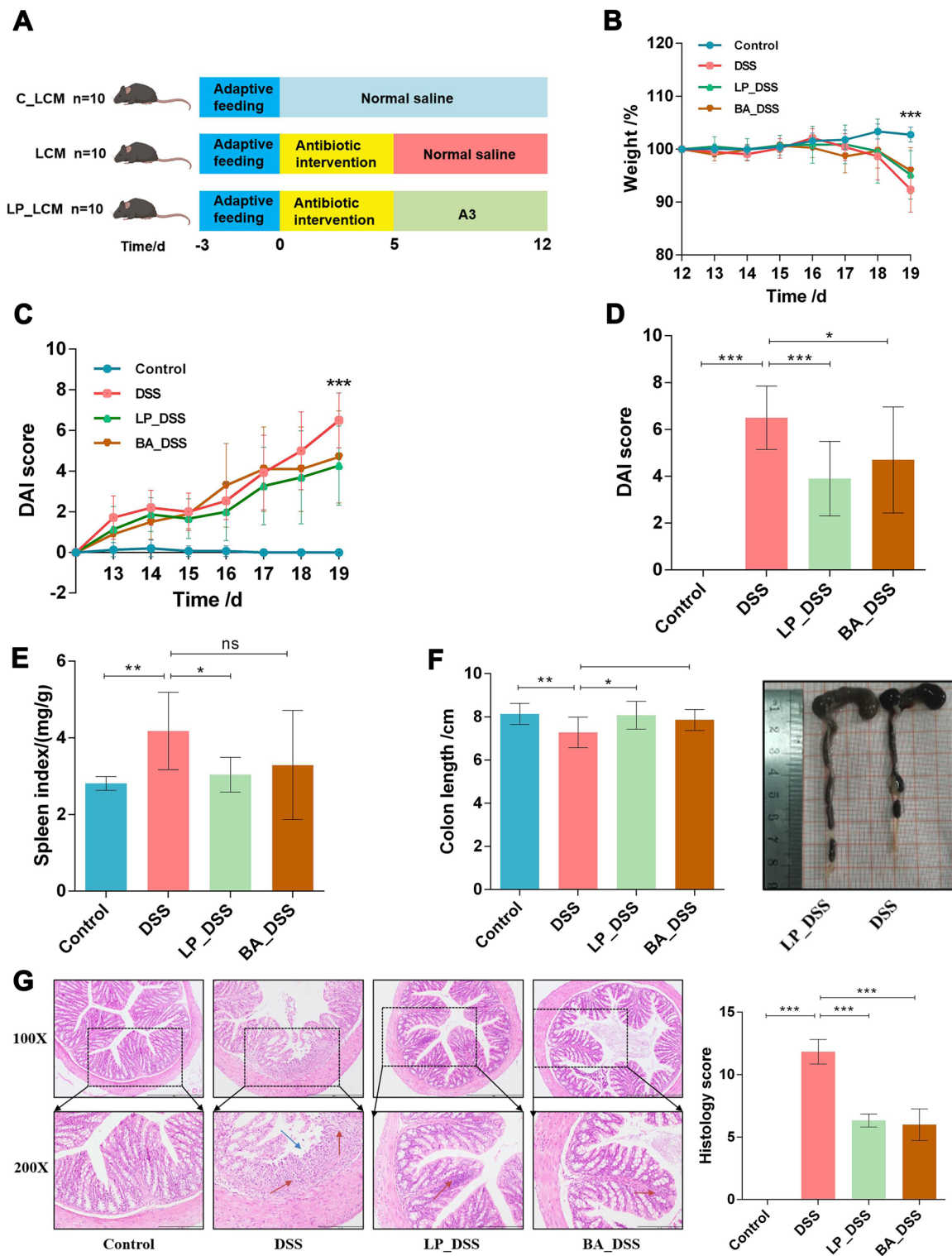
Fig. 2 *Lactobacillus plantarum* A3 can alleviate the clinical symptoms of ulcerative colitis in mice with gut microbial dysbiosis. **A** Mouse model of ulcerative colitis in mice with gut microbial dysbiosis; **B** Weight changes; **C** Changes in DAI score; **D** DAI index of mice in each group after 7 days of DSS intervention; **E** Spleen index changes; **F** Colon length changes among the four groups, and the colon morphology of DSS group and DSS group mice; **G** H&E staining results and histology scores, the red arrow points to the infiltration of inflammatory cells, the blue arrow points to the shedding of mucosal epithelial cells; $^{ns}p > 0.05$, $^*p < 0.05$, $^{**}p < 0.01$, $^{***}p < 0.001$; n = 10

Qin *et al. Animal Diseases*   (2023) 3:16

Page 5 of 18

the control group, a large number of inflammatory cells invaded the mucosal and submucosal layers of the colonic tissue, and many colonic mucosal epithelial cells detached in the DSS group. After treatment with *Lactobacillus plantarum* A3 or butyrate, no colonic mucosal epithelial cell detachment was observed in colonic tissue, but some colonic mucosal and submucosal layers still had inflammatory cell invasion, and the pathological score was also significantly decreased ($p < 0.001$) (Fig. 2G), suggesting that *Lactobacillus plantarum* A3 can reduce DSS damage to colonic tissue.

Lactobacillus plantarum A3 can regulate the serum biochemical indexes of mice

Serological parameters can often more intuitively illustrate the degree of damage to body cells. Thus, we studied the serum biochemical indexes in each group. The results showed that, compared with the control group, both MPO and MDA were significantly upregulated ($p < 0.001$), but SOD was significantly downregulated ($p < 0.001$) in the DSS group. Compared with the DSS group, MPO and MDA in the LP_DSS group were significantly decreased ($p < 0.05$), while SOD was significantly increased ($p < 0.05$) (Fig. 3A-C), and the concentration was closer to the control mice. This indicated that *Lactobacillus plantarum* A3 alleviated the degree of cell damage in mice.

Lactobacillus plantarum A3 can regulate cytokines expressed in mouse colon tissue

Inflammation in the body is often accompanied by changes in inflammatory cytokines. In DSS-induced mice, the expression of anti-inflammatory cytokine such as IL-1β, IL-6, TNF-α and IFN-γ were significantly increased at the gene level ($p < 0.001$) (Fig. 3D-G), while anti-inflammatory cytokine like IL-10 were significantly decreased ($p < 0.001$) (Fig. 3H). In addition, Foxp3, the main regulator of Treg cells, was also significantly increased ($p < 0.05$) (Fig. 3I). These showed that DSS promotes the inflammatory response at the gene level. When *Lactobacillus plantarum* A3 was involved in the regulation, IL-1β, IL-6, TNF-α and IFN-γ were significantly decreased at the gene level ($p < 0.05$) (Fig. 3D-G), while IL-10 increased significantly, rather than decreased ($p < 0.001$) (Fig. 3H). Besides, A3 significantly upregulated the expression of Foxp3 ($p < 0.001$) (Fig. 3). In summary, *Lactobacillus plantarum* A3 can inhibit the progression of inflammatory responses at the gene level.

The expression of these cytokines at the protein level were also interrogated by western blot, which was consistent with their trend at the gene level (Fig. 4A-D), indicating that DSS can promote the inflammatory response of mice at both the gene and protein levels.
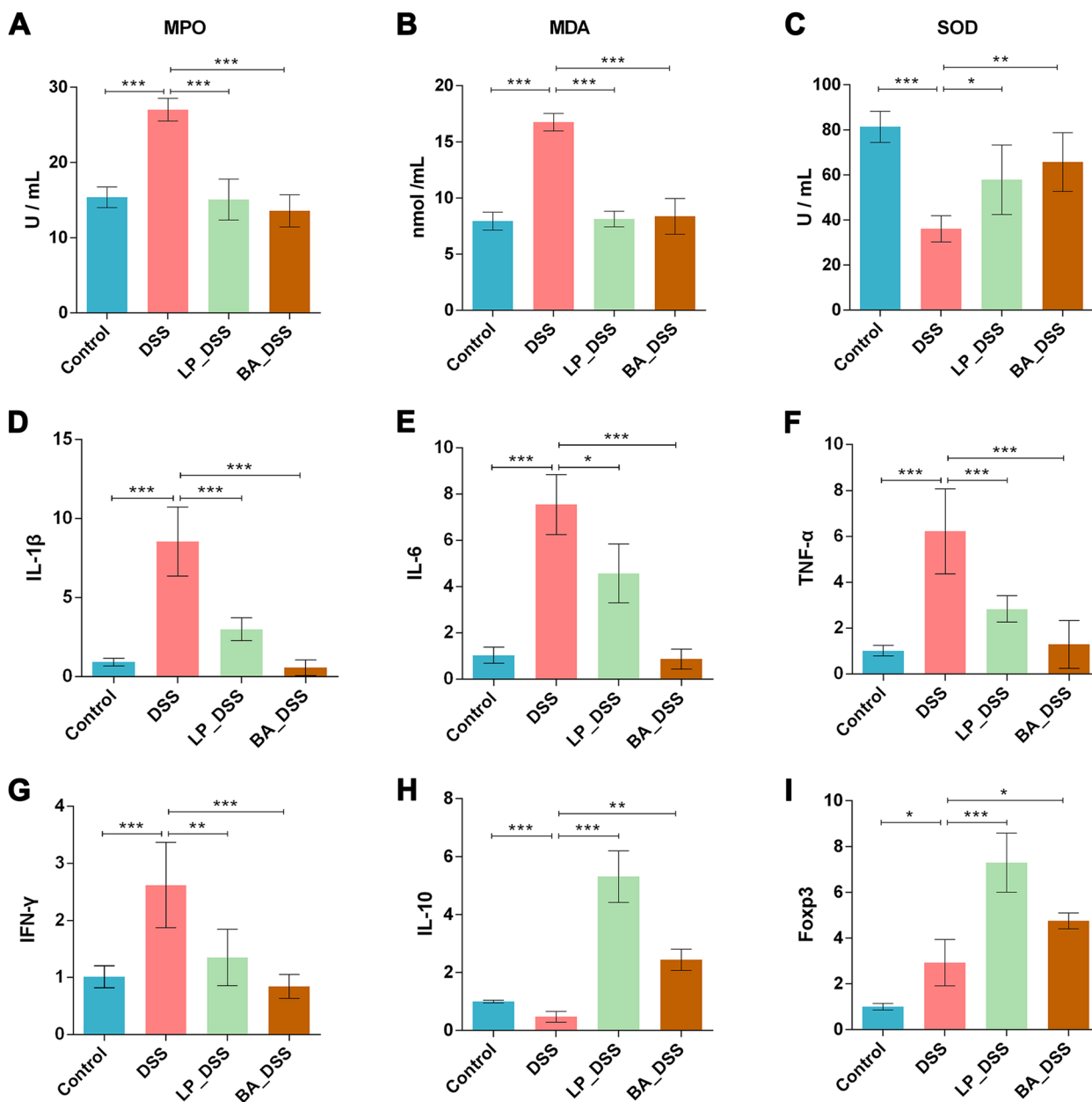
Similarly, *Lactobacillus plantarum* A3 can inhibit the inflammatory response at gene and protein levels.

To further explore the expression of Foxp3 at the protein level, immunohistochemical analysis was performed (Fig. 4F). Distribution of the brownish yellow positive signals indicated that Foxp3 was mostly expressed in the mucosa and submucosa of the colon. After DSS inducing, the mean optical density (MOD) of Foxp3 in colon tissue increased significantly ($p < 0.05$), which means that its expression increased. When mice were treated with *Lactobacillus plantarum* A3, the expression of Foxp3 in their colonic tissue was further increased ($p < 0.001$). These results showed that DSS induced a feedback regulatory immune response in mice, while *Lactobacillus plantarum* A3 further enhanced the immune response.

Lactobacillus plantarum A3 regulates the colonic microbiota in mice

To investigate the regulatory effect of *Lactobacillus plantarum* A3 on UC in mice with gut microbial dysbiosis, a high-throughput gene sequencing of 16S rDNA was performed in the colonic content microbiota in each group of mice. For the alpha diversity, compared with the DSS group, the Shannon and Simpson indexes of colonic content microbiota increased significantly in the LP_DSS group ($p < 0.001$), but the Chao 1 index did not increase significantly ($p > 0.05$) (Fig. 5A). These results showed that A3 can significantly restore the community diversity of intestinal microorganisms in mice, but its restoration effect on community richness is limited (Dill-McFarland et al. 2019; He et al. 2017). For the beta diversity, compared with the DSS group, Bray-curtis, unweighted UniFrac and weighted UniFrac distances were significantly changed in the LP_DSS group ($p < 0.01$) (Fig. 5B, Table S3), which indicated that *Lactobacillus plantarum* A3 could significantly affect intestinal bacteria in the colon of mice.

To further investigate which bacterium was specifically regulated by *Lactobacillus plantarum* A3, we conducted an analysis between the DSS group and LP_DSS group were conducted. At the phylum level, the four phyla with the highest abundance of colonic contents in the two groups were *Bacteroides*, *Firmicutes*, *Proteobacteria* and *Verrucomicrobia*. The relative abundance of each phylum was 63.80, 14.40, 15.77 and 6.03% in the DSS group, and 50.38, 22.84, 16.64 and 10.14% in the LP_DSS group (Fig.5, C). The results showed that A3 was involved in regulating each phylum. At the genus level, *Bacteroides* (63.80%), *Enterobacter* (9.32%) and *Blautia* (8.26%) were the top three microbiota in the DSS group, *Bacteroides* (50.38%), *Enterobacter* (15.33%) and

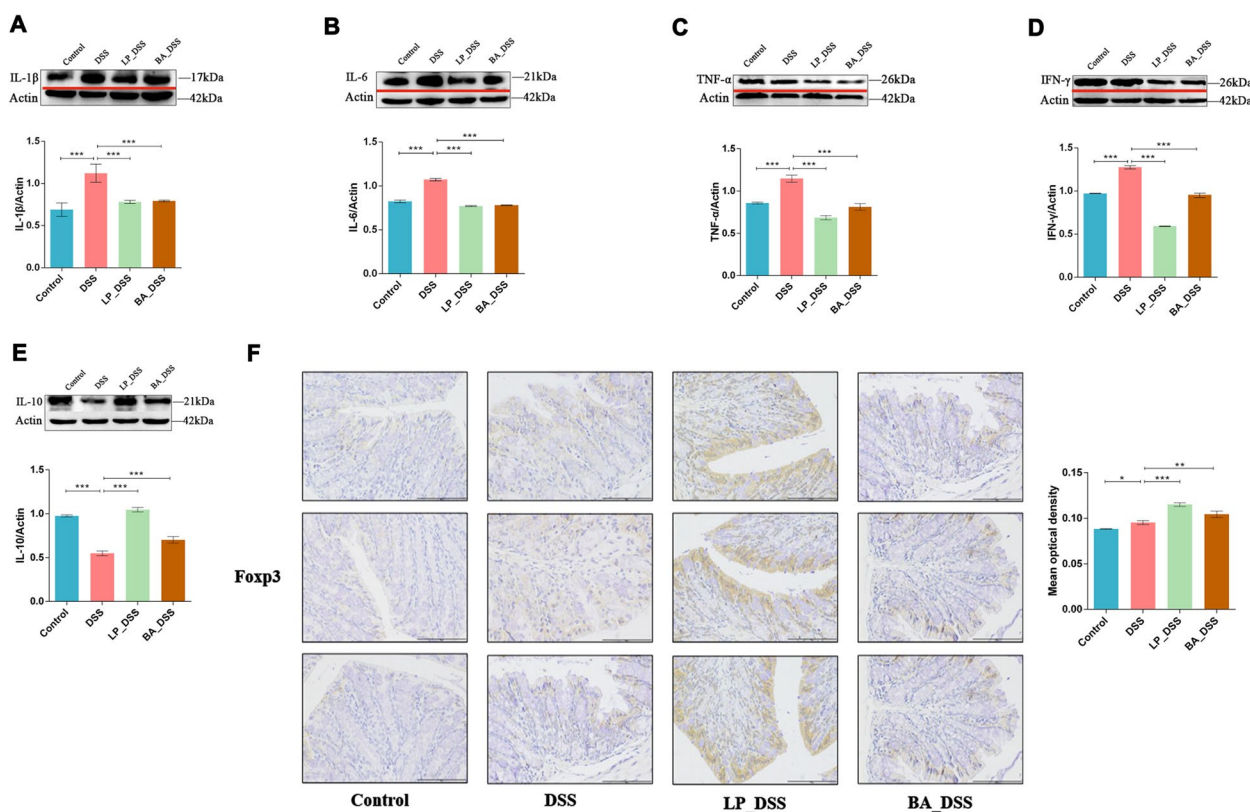Qin *et al. Animal Diseases*   (2023) 3:16

Page 6 of 18

Fig. 3 *Lactobacillus plantarum* A3 can regulate the biochemical indexes and cytokine gene expression of ulcerative colitis in mice with gut microbial dysbiosis. **A-C** Serum biochemical indexes (**A**: MPO; **B**: SOD; **C**: MDA); **D-I** Cytokine gene expression level in colonic tissue (**D**: IL-1β; **E**: IL-6; **F**: TNF-α; **G**: IFN-γ; **H**: IL-10; **I**: Foxp3); *$p < 0.05$, **$p < 0.01$, ***$p < 0.001$; n = 10

Akkermansia (10.14%) were the top three microbiota in the LP_DSS group which meant that *Lactobacillus plantarum* A3 changed the microbiota with high abundance, which was consistent with the beta diversity analysis (Fig. 5D).

LEfSe confirm the specific bacteria that had significant changes between the two groups. At the phylum level, the abundance of *Firmicutes* and *Verrucomicrobia* was significantly upregulated in the LP_DSS group ($p < 0.05$)

compared with the DSS group, but *Bacteroidetes* was significantly downregulated ($p < 0.05$) (Fig. 5E). At the genus level, the abundance of *Blautia*, *Akkermansia*, *Citrobacter* and *Flexispira* was significantly upregulated ($p < 0.05$) in the LP_DSS group, but *Bacteroides* was significantly downregulated ($p < 0.05$) (Fig. 5F). In general, *Lactobacillus plantarum* A3 treatment significantly transformed the diversity and composition of gut microbiota.
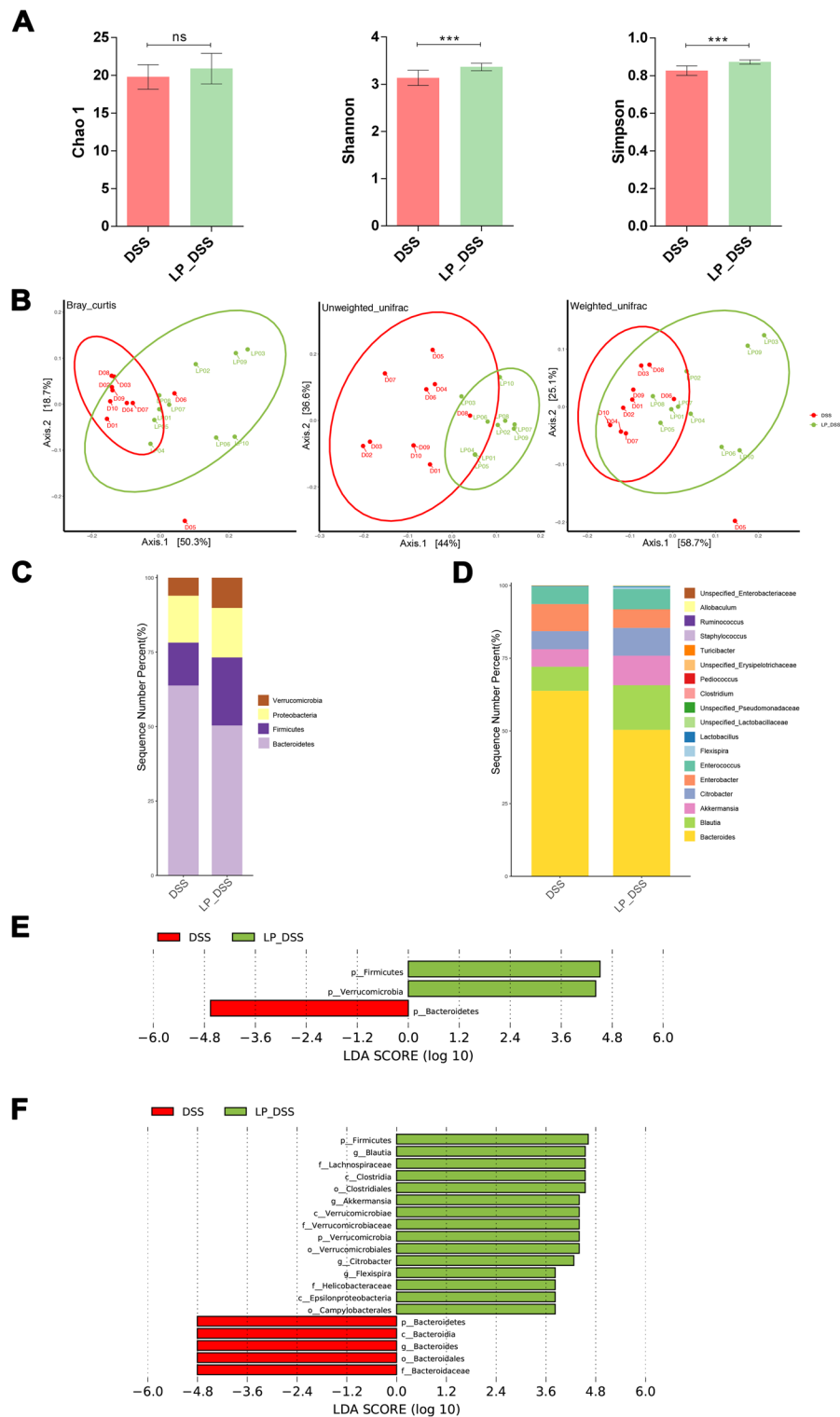
Fig. 4 *Lactobacillus plantarum* A3 can regulate the biochemical indexes and cytokine expression of ulcerative colitis in mice with gut microbial dysbiosis. **A-E** Expression of cytokines at protein level in colonic tissue was measured by western blot in each group (**A**: IL-1β; **B**: IL-6; **C**: TNF-α; **D**: IFN-γ; **E**: IL-10); **F** Foxp3 in colonic tissue was measured by immunohistochemistry, and the mean optical density was calculated in each group. *$p < 0.05$, **$p < 0.01$, ***$p < 0.001$

Lactobacillus plantarum A3 can regulate changes of colonic metabolites in mice

Untargeted metabolomic analysis can detect small molecule metabolites with a relative molecular weight of less than 1000 in the sample, from which we can obtain differential metabolites and metabolic pathways between the DSS group and the LP_DSS group. We used PCA to model each sample and found that there were no outlier points in the intragroup samples under both positive and negative polarity modes, which indicated that there was little difference in the intragroup samples and could be used for the analysis of differential metabolites (Fig. 6A-D). The factors that can distinguish sample grouping to the greatest extent can be found using PLS-DA, and the overfitting caused by the PLS-DA model can be improved using OPLS-DA. Therefore, we plotted the scatter diagram with the two best discriminating factors and found that the sample point clouds of the DSS group and the LP_DSS group were distributed in different regions, which indicated that the PLS-DA model and the OPLS-DA model had better discrimination effects (Fig. 6E-H), and there should be

metabolites with significant differences between the two groups.

Then, according to the above discriminant analysis model, the metabolites that play an important role in the discrimination process are analyzed. These metabolites have the potential to be used as biomarkers between the two groups. Value importance in projection (VIP) > 1 was as the standard and screened 383 metabolites in positive polarity mode and 285 metabolites in negative polarity mode. To further explore the differential metabolites, univariate analysis were also performed. $p < 0.05$ and fold change (FC) > 2 were used as the screening criteria. The results showed that, compared with the DSS group, there were 23 metabolites with more than 2 FC in the LP_DSS group ($p < 0.05$) in the positive polarity mode, of which arachidonoyl ethanolamide phosphate guanosine (AEA-P) had the highest fold upregulation, reaching 28.70 FC ($p < 0.001$), and four metabolites including serilin and Cortisone were also upregulated by more than 10 FC ($p < 0.001$) (Fig. 6I, Table 1). In the negative polarity mode, there were nine metabolites with

Fig. 5 *Lactobacillus plantarum* A3 can regulate the gut microbiota of ulcerative colitis in mice with gut microbial dysbiosis. **A** Alpha diversity of colon contents in mice, $^{ns}p > 0.05$, ***$p < 0.001$. **B** Beta diversity of colon contents in mice. **C** Bar plots of the phylum taxonomic levels in the DSS and LP_DSS groups; **D** Bar plots of the genus taxonomic levels in the DSS and LP_DSS groups; **E-F** Difference in dominant microorganisms of colon contents between the DSS group and LP_DSS group via distribution histogram based on LDA. The criteria for feature selection was log LDA score > 2.0 (E: at the phylum level; F: at the genus level)
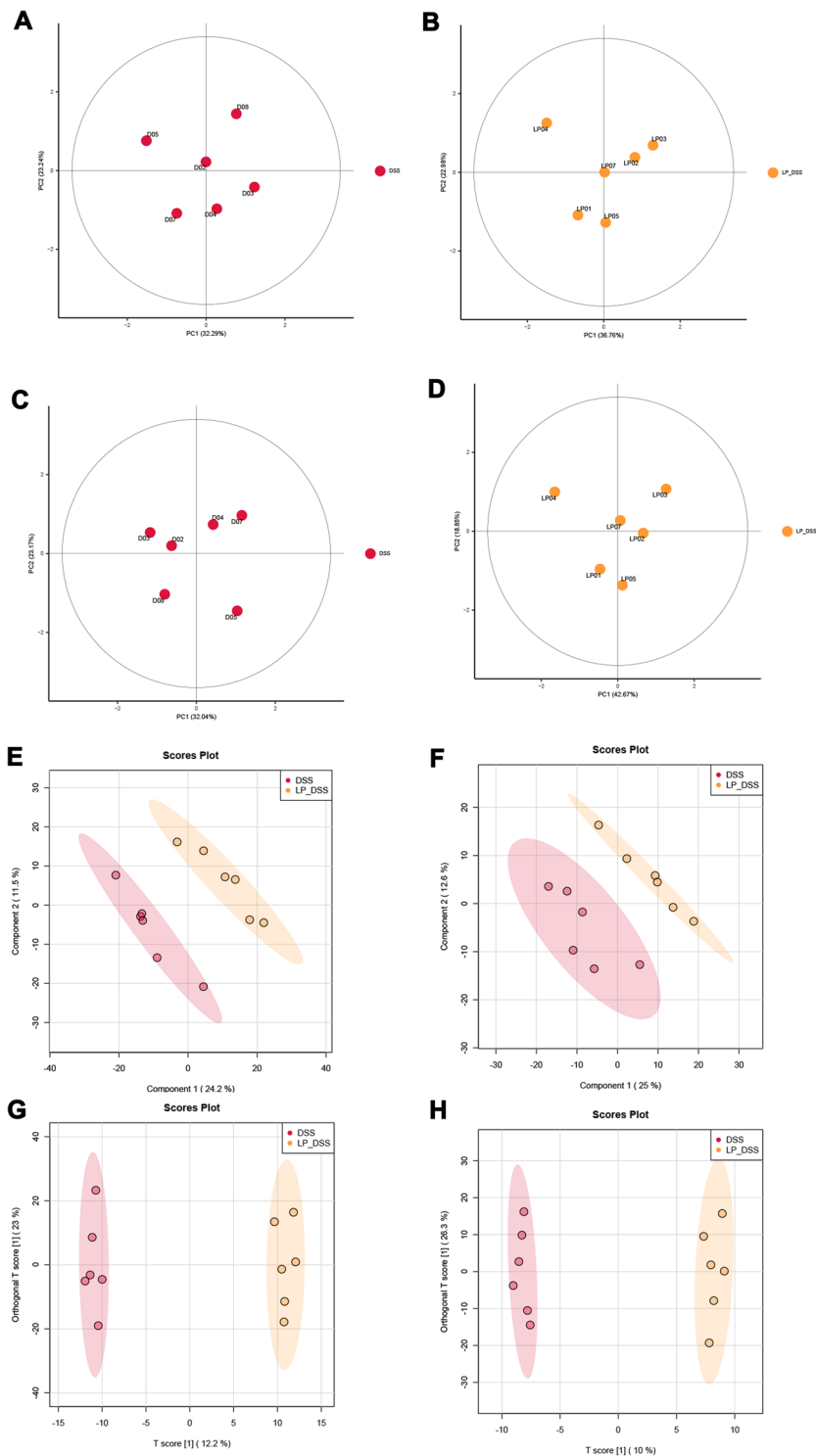
Fig. 6 *Lactobacillus plantarum* A3 can regulate the metabolite changes of colon contents in ulcerative colitis in mice with gut microbial dysbiosis. **A-D** PCA score diagram (**A**-**B**: under positive polarity mode; **C-D**: under negative polarity mode). **E-F** Scatter diagram of PLS-DA models (**E**: under positive polarity mode; **F**: under negative polarity mode); **G-H** Scatter diagram of OPLS-DA models and OPLS-DA models (**G**: under positive polarity mode; **H**: under negative polarity mode). **I-J** Univariate analysis of differential metabolites in mouse colonic contents between the DSS group and LP_DSS group (**I**: under positive polarity mode; **J**: under negative polarity mode), log2(FC) > 0 represents metabolites with high abundance in the LP_DSS group. **K-L** The metabolic pathways of differential metabolite enrichment by ORA (K: under positive polarity mode; L: under negative polarity mode)

Qin *et al. Animal Diseases*   (2023) 3:16

Page 10 of 18
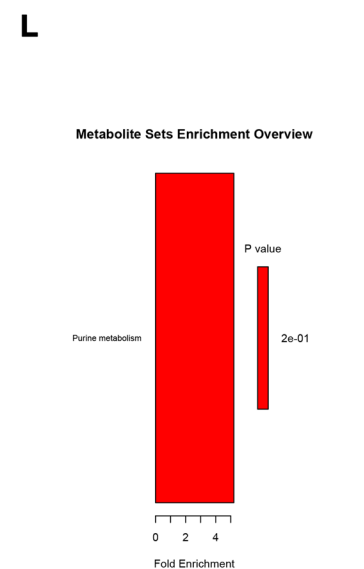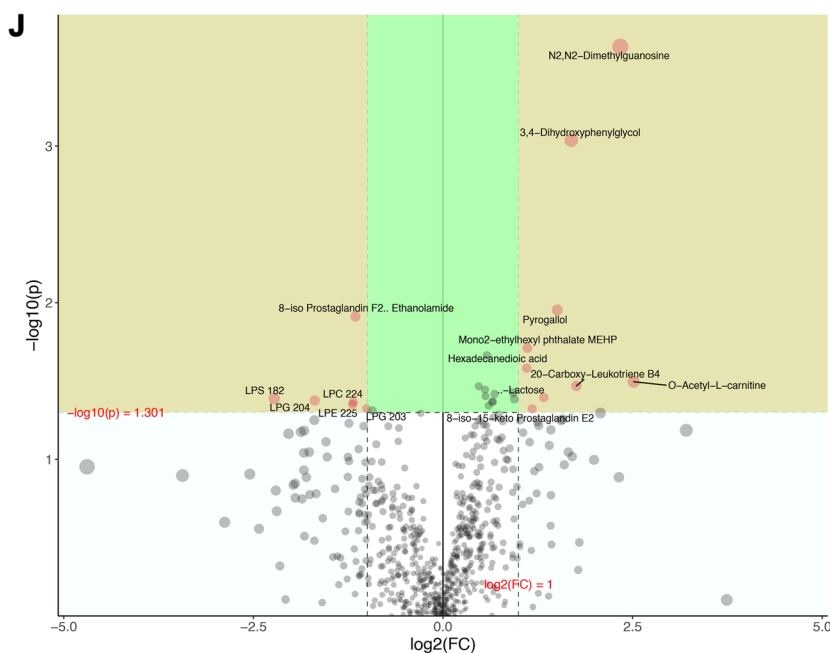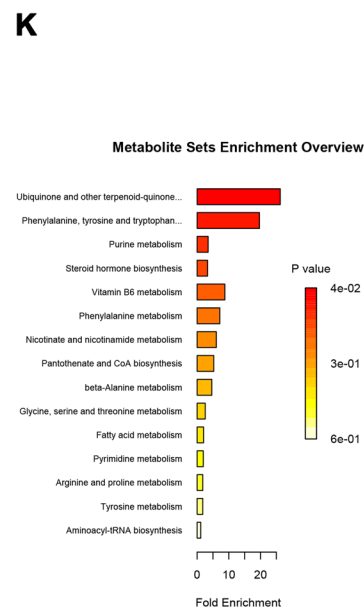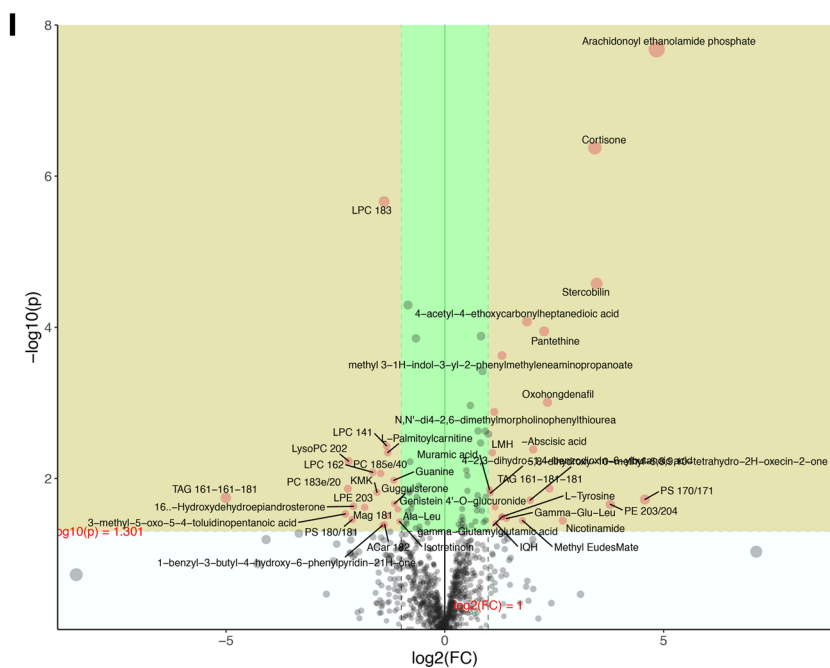
Fig. 6 continued

more than 2 FC upregulation in the LP_DSS group, and the two metabolites with the highest upregulation were O-LPL-carnitine ($p < 0.05$, 5.712-fold) and N2, N2-dimyl ($p < 0.001$, 5.06-fold) (Fig. 6J, Table 2). Enrichment analysis can help us find pathways with key roles and thus can predict the molecular mechanisms of the entire regulatory process. Based on the metabolites that were significantly different between the DSS group and the LP_DSS group (*t* test, $p < 0.05$), we looked for the metabolic pathways in which these metabolites appeared and calculated the *p* value and fold enrichment of ORA for these metabolic pathways (Fig. 6K-L). Impact can be calculated by topological analysis to judge the magnitude of the effect

Table 1 Differential metabolites in mouse colonic contents between the DSS group and LP_DSS group under positive polarity mode (screening criteria: VIP > 1; $p < 0.05$; FC > 2)

Differential metabolites	VIP	p	FC
Arachidonoyl ethanolamide phosphate	2.810	<0.001	28.70
PS 170/171	1.945	0.0190	23.80
PE 203/204	1.808	0.0220	13.77
Stercobilin	2.652	<0.001	11.09
Cortisone	2.779	<0.001	10.77
Nicotinamide	1.792	0.0360	6.486
TAG 161-181-181	1.893	0.0136	5.250
Oxohongdenafil	2.377	<0.001	5.087
Pantethine	2.499	<0.001	4.827
Abscisic acid	2.189	0.0041	4.060
5,8-dihydroxy-10-methyl-5,8,9,10-tetrahydro-2H-oxecin-2-one	1.922	0.0194	3.866
4-acetyl-4-ethoxycarbonylheptanedioic acid	2.591	<0.001	3.677
Methyl EudesMate	1.787	0.0360	3.423
Gamma-Glu-Leu	1.803	0.0340	2.657
L-Tyrosine	1.761	0.0320	2.490
methyl 3-1H-indol-3-yl-2-phenyl-methyleneaminopropanoate	2.465	<0.001	2.476
gamma-Glutamylglutamic acid	1.807	0.0327	2.456
IQH	1.677	0.0392	2.240
Genistein 4′-O-glucuronide	1.812	0.0240	2.219
N, N′-di4-2,6-dimethylmorpholinophenylthiourea	2.350	0.0013	2.192
LMH	2.205	0.0046	2.128
4-2,3-dihydro-1,4-benzodioxin-6-ylb-utanoic acid	1.932	0.0157	2.060
Muramic acid	2.004	0.0140	2.030

Add notes: *VIP* value importance in projection, *FC* fold change

Table 2 Differential metabolites in mouse colonic contents between the DSS group and LP_DSS group under negative polarity mode (screening criteria: VIP > 1; $p < 0.05$; FC > 2)

Differential metabolites	VIP	p	FC
O-Acetyl-L-carnitine	2.800	0.0319	5.712
N2, N2-dimethylguanosine	2.658	<0.001	5.057
20-Carboxy-Leukotriene B4	2.226	0.0340	3.386
3,4-Dihydroxyphenylglycol	2.010	<0.001	3.233
Pyrogallol	2.176	0.0111	2.843
W-Lactose	2.187	0.0402	2.513
8-iso-15-keto Prostaglandin E2	2.109	0.0476	2.259
Mono2-ethylhexyl phthalate MEHP	2.100	0.0194	2.163
Hexadecanedioic acid	1.998	0.0262	2.150

Add notes: *VIP* value importance in projection, *FC* foldchange

of metabolites in metabolic pathways. Combined enrichment and topological analysis, using $p < 0.05$ and Impact >0.2 as criteria, metabolic pathways significantly affected by differential metabolites from the above metabolic pathways were selected: ubiquinone and other terpenoid-biosynthesisu (impact = 0.5, $p < 0.05$, fold enrichment = 26.24), phenylalanine, tyrosine and tryptophan (impact = 0.25, $p < 0.05$, fold enrichment = 19.68). The above results showed that *Lactobacillus plantarum* A3 affected not only the changes of metabolites in the mouse colon, but also the metabolic pathway.

Discussion

Recent studies have found that early gut microbiota imbalance can increase the incidence of diseases such as asthma (Arrieta et al. 2015), IBD (Hviid et al. 2011) and immune diseases (Round and Mazmanian 2009). However, antibiotics are not only inevitably used in clinical treatment, but have also become one of the most widely used drugs (Adriaenssens et al. 2011; Vaz et al. 2014). Therefore, restoring antibiotic-induced gut microbiota imbalance and preventing related diseases is a key problems. UC is an idiopathic inflammatory bowel disease. Its high incidence and lack of specific drugs are the reasons why it has become a problem in modern medicine (Fan et al. 2019). Although the etiology is unknown, the phenomenon of gut microbial dysbiosis has been proven to appear before UC (Wu et al. 2020). In addition, when mice were first treated with antibiotics, the stability of gut microbiota was destroyed, their sensitivity to DSS increased, and finally, the symptoms of ulcerative colitis were more serious (Ozkul et al. 2020). This suggests that timely treatment and restoration of the stability of gut microbiota after gut microbial dysbiosis may reduce IBD's incidence or symptoms.

As a kind of probiotic, *Lactobacillus* has been proven to maintain and restore the homeostasis and stable heredity of gut microbiota (Ma et al. 2020), and it also has a certain therapeutic effect on IBD (including UC and CD) (Guo et al. 2019; Wang et al. 2020). *Lactobacillus plantarum* A3 is a lactobacillus that has good probiotic characteristics isolated and screened from healthy adult horses, and it has a certain alleviating effect on UC in mice (Qin et al. 2022), Therefore, in this study, we used *Lactobacillus plantarum* A3 as the main therapeutic drug to explore its regulatory effect on colitis in mice with gut microbial dysbiosis. In addition, as a short chain fatty acid (SCFA), butyrate can not only be the main energy source of colonic epithelial cells, but also regulate epithelial stem cells (Kaiko et al. 2016), and promote epithelial homeostasis together with other SCFAs (Macia et al. 2015). Therefore, when

Qin *et al. Animal Diseases* (2023) 3:16

Page 12 of 18

constructing the mouse UC model, we used butyrate as a positive control of treatment.

In the first stage, lincomycin hydrochloride was used to establishe a mouse model of gut microbial dysbiosis. In clinical practice, lincomycin hydrochloride is commonly used to treat various bacterial infections. It can inhibit the growth of bacteria by inhibiting the synthesis of proteins in bacteria, and it has strong antibacterial and bactericidal effects on Gram-positive bacteria, especially anaerobic bacteria (Geddes et al. 1964). Recent studies have shown that short-term overdose of lincomycin hydrochloride can lead to microbiota imbalance, intestinal tissue damage and immune function decline in mice (Li et al. 2019; Lv et al. 2017). Therefore, lincomycin hydrochloride was used as an intervention drug, and its effect on each gut microbiota of mice was explored. The results showed that lincomycin hydrochloride had no significant effect on the microbiota of the small intestine in mice, but it had a significant damage on the microbiota of the large intestine, not only the number, but also the structure.

Based on the constructed mouse gut microbial dysbiosis model, we induced UC in mice with DSS and explored the regulatory effect of *Lactobacillus plantarum* A3. UC often requires some specific indicators to evaluate, such as spleen index, colon length and DAI index. Splenomegaly is one of the common symptoms in UC mice (Zhang et al. 2017). Colon length and DAI index are often used to evaluate the severity of ulcerative colitis in clinical diagnosis and treatment (El Sayed and Sayed 2019). In addition, pathological tests are often used as one of the gold standards for diagnosing the symptoms of ulcerative colitis (Allen et al. 2012; Meira et al. 2008). After DSS induction, the spleen index and DAI index of mice were significantly increased ($p < 0.05$), and the colon was significantly shortened ($p < 0.05$). H&E staining showed that there were a large number of inflammatory cells in the mucosal layer and submucosal layer in the colon tissue, accompanied by a large number of mucosal epithelial cells falling off. The above results showed that DSS successfully induced ulcerative colitis in mice with gut microbial dysbiosis. When mice were treated with *Lactobacillus plantarum* A3, the spleen index and DAI index of mice decreased significantly ($p < 0.05$), the colon length was closer to that of the control group, and H&E staining showed that the degree of inflammatory cell invasion decreased significantly. The above results showed that *Lactobacillus plantarum* A3 could alleviate the clinical symptoms of ulcerative colitis in mice with gut microbial dysbiosis.

Oxidative stress is closely related to ulcerative colitis. MDA is the end product of the peroxidation reaction between free radicals and lipids. It reflects the degree of lipid peroxidation in the body. SOD is an antioxidant enzyme, that can catalyze free radicals into oxygen and hydrogen peroxide (Yu et al. 2020; Li et al. 2023). Therefore, the contents of MDA and SOD in the body are often negatively correlated. Our study showed that *Lactobacillus plantarum* A3 could significantly upregulate the level of SOD and downregulate the level of MDA ($p < 0.05$), indicating that they can play a regulatory role through antioxidation.

At present, it is generally believed that patients with UC have intestinal mucosal inflammation and immune abnormalities (Medzhitov 2008). MPO exists in neutrophils, and its activity is directly proportional to the population of neutrophils in the inflammatory area (Bastaki et al. 2018). Therefore, the significantly increased content of MPO in the DSS group also suggested the presence of excessive neutrophil invasion in mice, which was consistent with the results of H&E staining in colon tissue. The aggravation of oxidative stress and the increase of neutrophils in the body can further stimulate the release of immune cytokines associated with UC (Leppkes and Neurath 2020). For example, oxidative stress can not only stimulate macrophages to release IFN-γ, but also induce the release of TNF-α, IL-6, IL-1β and other inflammatory factors, further causing intestinal mucosal metabolic disorders and intestinal mucosal inflammatory immune disorders, which can lead to systemic inflammatory response syndrome and multiple organ dysfunction (Li et al. 2021a, 2021b, 2021c; Vlahakos et al. 2012). In our study, the expression levels of IFN-γ, TNF-α, IL-6, and IL-1β in the DSS group were significantly higher than those of the control group at both gene and protein levels ($p < 0.001$), which indirectly indicated abnormalities in intestinal mucosal inflammation and immune response in mice. As an anti-inflammatory cytokine, IL-10 can inhibit the secretion of proinflammatory cytokines such as IFN-γ, TNF-α, IL-6 and IL-1β, regulate the differentiation and proliferation of macrophages, T cells and B cells, inhibit Th1/Th17 responses, which are essential for intestinal immune homeostasis (Bárcena et al. 2019). *Lactobacillus plantarum* A3 promoted the expression of IL-10 and inhibited IL-1β, IL-6, TNF-α and IFN-γ, which further proved that it can effectively regulate intestinal inflammation and intestinal immune response in mice. Foxp3 is considered to be a specific transcriptional marker of CD4^{+}CD25^{+} regulatory T cells (CD4^{+}CD25^{+} Treg), which plays an important role in the proliferation, differentiation and immune function of Treg cells (Jia et al. 2020; Zhou et al. 2020). Moreover, recent studies have also shown that the expression of Foxp3 is positively correlated with the expression of programmed cell death ligand (PD-L1), and PD-L1 mediated signal transduction pathway is one of the main processes regulating intestinal

local inflammatory response (Yamamoto et al. 2022). This illustrated that *Lactobacillus plantarum* A3 can regulate the immune response and inflammatory response of mouse intestine by upregulating Foxp3.

The severity of UC is related to the decline in the diversity of intestinal microorganisms, such as the relative decrease in the abundance of *Clostridium* and *Akkermansia* (Pittayanon et al. 2020; Zhou et al. 2018), which is consistent with the changes in the DSS group in our study. *Lactobacillus plantarum* A3 significantly restored the alpha diversity and beta diversity of intestinal microorganisms in mice ($p < 0.05$), regulated the microbiota structure, and increased the relative abundance of *Blautia*, *Akkermansia*, *Citrobacter* and *Flexispira*. *Blautia* is an anaerobic bacterium with probiotic characteristics. According to the analysis of phenotype and phylogeny, some species of *Clostridium* and *Ruminococcus* have been reclassified to this genus. *Blautia* plays an important role in regulating the growth of gut microbiota and inflammation. This is mainly because *Blautia* has the ability to produce bacteriocin, which makes it have the potential to inhibit the colonization of pathogenic bacteria in the intestine, especially *Clostridium perfringens* and vancomycin-resistant *enterococci* (Liu et al. 2021; Li et al. 2021a, 2021b, 2021c). In addition, *Blautia* plays an important role in obesity related diseases. It is the only bacterium negatively related to visceral fat accumulation (Ozato et al. 2019; Song et al. 2014). As a mucin decomposing bacterium in the body, *Akkermansia* widely exists in the intestinal tract of animals. It obtains a competitive advantage by improving the utilization rate of mucin in the body, so it can be highly colonized in the intestinal tract, and it can alleviate the inflammatory reaction by reducing the permeability of the intestinal tract and the infiltration derived pro-inflammatory lipopolysaccharide (Bárcena et al. 2019; Depommier et al. 2019; Kim et al. 2022). *Citrobacter* and *Flexispira* are common microbiota in the intestine. There are few studies on their relationship with UC. Some studies have intervened with *Citrobacter rodentium* to induce colitis in mice and found that it can reduce the weight of mice and cause diarrhea (Bhinder et al. 2013). However, in our study, it was not found that after the intervention of *Lactobacillus plantarum* A3, the weight of mice was less than that of the DSS group and there was no diarrhea, which indicated that not all *Citrobacter* can induce disease. The limitations of the genus level made it impossible for us to further analyze it, which also provided a new idea for our future research. In general, *Lactobacillus plantarum* A3 had the ability to regulate gut microbiota in mice. It not only increased the diversity of gut microbiota, but also further regulated the inflammatory response in vivo by upregulating the abundance of beneficial bacteria such as *Blautia* and *Akkermansia*.

Intestinal metabolites can regulate the intestinal environment together with gut microbiota. Compared with the DSS group, the colonic metabolites in the LP_DSS group were significantly changed, with the highest upregulation of arachidonoyl ethanolamide phosphate (AEA-P), reaching 28.70-fold ($p < 0.001$). AEA-P is a newly discovered endogenous lipid, a precursor of arachidonoyl ethanolamide (AEA), and its function is similar to AEA. As an "endocannabinoid" (which has similar pharmacological effects to the active ingredient of cannabis: Δ^9-tetrahydro-cannabinol), AEA is often released from depolarized neurons, endothelial cells, and macrophages in the body, and then participates in cellular activities as an endogenous ligand for cannabinoid receptors in the central nervous system (CB1 subtype) and peripheral immune cells (CB2 subtype). Besides, it can be selectively absorbed by cells, and then degraded by fatty acid amide hydrolase (FAAH) to ethanolamine and arachidonic acid (AA), further playing an anti-inflammatory role. It is worth mentioning that AEA can also reduce pain at the site of tissue injury (Maccarrone et al. 2000). These may be the reasons for the significant upregulation of AEA-P concentration in group A mice. In addition, *Lactobacillus plantarum* A3 also increased the concentrations of cortisone in the colon of mice by 10.77-fold ($p < 0.001$). Cortisone is a type of glucocorticoid, that was used to treat IBD as early as 1955 (Singh 2018). It can regulate cytokines in the body, such as inhibiting the release of pro-inflammatory cytokines IL-6, IFN-γ and TNF-α, while stimulating the production of anti-inflammatory cytokine IL-10, which shows that the increase in cortisone concentration is also one of the reasons for the changes of cytokine in mice. Today, there are still studies on synthetic cortisone analoges for improving the stability of drugs and optimizing their efficacy in treating IBD (Rol et al. 2021). Therefore, the reason why *Lactobacillus plantarum* A3 induced a significant increase in intestinal cortisone might be one of the priorities in further research. Through enrichment analysis and topological analysis, it was also found that *Lactobacillus plantarum* A3 significantly affects ubiquinone and other terpenoid quinone biosynthesis, phenylalanine, tyrosine and tryptophan biosynthesis. These pathways predict the intestinal metabolic activities that *Lactobacillus plantarum* A3 may have participated in. In further studies, we can explore the specific mechanism by which *Lactobacillus plantarum* A3 regulats UC in mice with gut microbial dysbiosis by verifying these metabolic pathways.

Qin *et al. Animal Diseases*   (2023) 3:16

Page 14 of 18

Conclusion

In this study, we successfully constructed a gut microbial dysbiosis model in mice by lincomycin hydrochloride and found that it had a more significant destructive effect on the microbiota of the large intestines. Subsequently, we constructed a UC model on the basis of gut microbial dysbiosis in mice and found that *Lactobacillus plantarum* A3 could alleviate the clinical symptoms of mice and achieve a mitigatory effect by regulating the expression of cytokines, affecting the structure of gut microbiota and regulating the level of intestinal metabolites.

Methods

Animals

Five-week-old male C57BL/6 mice were obtained from the animal center of Huazhong Agricultural University (Wuhan, China). They were housed under specific pathogen-free conditions and had access to food and water ad libitum at a temperature of $25\pm2℃$, relative humidity of 40-60% (12:12-hour light/dark cycle). All animal experimental protocols (HZAUMO-2021-0068 and HZAUMO-2021-0138) were approved by the Ethics Committee of Huazhong Agricultural University (Wuhan, China) and performed following the guidelines of the National Institutes of Health Guide for the care and Use of Laboratory Animals.

Mouse model of gut microbial dysbiosis

C57BL/6 mice were randomly divided into two groups: the control-antibiotic group (C_LCM group) and the antibiotic intervention group (LCM group). The first 3 d, mice were adaptive feeding, and then, mice in the LCM group were given lincomycin hydrochloride (30 mg/10 g body weight) for 5 d. Mice in the C_LCM group were given normal saline as a control. After that, the mice were euthanized and the intestinal contents of duodenum, jejunum, ileum, cecum, colon and rectum were taken.

Mouse model of ulcerative colitis

C57BL/6 mice were randomly divided into four groups (n = 15): Control-DSS group (Control group), DSS group, *Lactobacillus plantarum* A3-DSS group (LP_DSS group) and butyrate-DSS group (BA_DSS group, as a positive control group). The experimental period was 22 d, in which the first 3 d were adaptive feeding. In the following 5 d, mice in the DSS group and LP_DSS group were intragastrically administered lincomycin hydrochloride (30 mg/10 g bodyweight). In the remaining 14 d, mice in the LP_DSS group were intragastrically administered *Lactobacillus plantarum* A3 (5×10^8 CFU/10 g bodyweight), mice in the BA_DSS group were intragastrically administered an equal volume of butyrate (30 mg/10 g bodyweight), and mice in the DSS group were intragastrically administered an equal volume of normal saline. Notably, on the last 7 d of the experiment, except for the control group, which maintained normal drinking water, the other three groups of mice were given drinking water containing 3% (*w*/*v*) DSS, in which freshly prepared DSS solution was changed every 2 d (Fig. 2A). At the end of the experiment, mice were euthanized, and serum, spleen tissue and colon tissue, colon contents were collected to subsequent studies.

Intestinal contents genomic DNA extraction and 16S-rRNA sequencing

The intestinal contents of mice in each group were subjected to total DNA extraction by the E.Z.N.A.® soil kit (Omega Biotek, Norcross, GA, U.S.). After ensuring the eligibility of the DNA, the V3-V4 variable region was amplified by PCR with 338F (5′-ACTCCTACGGGA GGCAGCAG-3′) and 806R (5′-GGACTACHVGGG TWTCTA AT-3′) primers, and the amplification program was: 95℃ for 3 min, 27 cycles (95℃ for 30 s, 55℃ for 30 s, 72℃ for 30 s), and 72℃ for 10 min. The resulting PCR products were purified using the AxyPrep DNA Gel Extraction Kit (Axygen Biosciences, Union City, CA, USA). Standard operating procedures for generating sequencing libraries from the purified amplified fragments. Then, purified amplicons were pooled in equimolar amounts and paired-end sequenced (2×300) on an Illumina MiSeq platform (Illumina, San Diego, USA). Quality control and species annotation were conducted by previous methods (Bokulich et al. 2018; Callahan et al. 2016). Any contaminating mitochondrial and chloroplast sequences were filtered using the QIIME2 feature-table plugin. Venn diagram was drawn to analyze the unique or common OTUs between different groups. Alpha diversity, including the Chao1, Shannon and Simpson indexes, was calculated to estimate the microbial diversity within an individual sample. Beta diversity, including BrayCurtis, weighted UniFrac and unweighted UniFrac was determined to investigate the structural variation in microbial communities across samples and then visualized *via* principal coordinate analysis (PCoA) (Vázquez-Baeza et al. 2013). Linear discriminant analysis effect size (LEfSe) was employed to identify the bacteria with different abundances among samples and groups (Segata et al. 2011).

Clinical indicator analysis

During the experiment, mental status, weight, fecal shape and fecal occult blood for mice were recorded every day. The disease activity index (DAI) was scored based on the weight loss rate, fecal score and occult blood score of

Qin *et al. Animal Diseases*   (2023) 3:16

Page 15 of 18

mice. The score range for each parameter is 0-4 points, and the sum for the parameters is the final score (up to 12 points) (Table S1) (Liu et al. 2020). After the mice were euthanized, the colon length and the weight of the mice in each group were measured, and the spleen index was calculated.

Histology
The colonic tissue sections of mice in each group were taken and the feces were washed with 0.9% sterile normal saline, fixed in 4% paraformaldehyde, dehydrated with ethanol, and processed into a paraffin-embedded block, cut into 5 μm sections, and stained with hematoxylin and eosin (H&E). Pathobiological slices were evaluated in a blinded manner, and the pathological scores were assessed based on the following parameters: inflammation, epithelial defects, crypt pathology, dysplasia/neoplasia and the area of dysplasia/neoplasia (scoring criteria in supplementary materials) (Allen et al. 2012; Meira et al. 2008).

Serum biochemical detection
Serum samples from mice were collected for biochemical index analysis. The activities of myeloperoxidase (MPO), and superoxide dismutase (SOD), along with the concentrations of malonaldehyde (MDA), were measured by specific assay kits (Nanjing Jiancheng Bioengineering Institute, Nanjing, PRC).

Gene expression analysis
Total RNA from colon tissue was extracted with a *Steady*-Pure Universal RNA Extraction Kit (AG21017, Accurate Biotechnology, Hunan, PRC). RNA was reverse transcribed into complementary DNA (cDNA) (*Evo M-MLV* RT Mix Kit with gDNA Clean for qPCR; AG11728, Accurate Biotechnology, Hunan, PRC). Real-time PCR (SYBR Green premix Pro Taq HS qPCR kit; AG11701, Accurate Biotechnology, Hunan, PRC) was used to detect gene expression and the $2^{-\Delta\Delta Ct}$ method was used for calculation and analysis. The primers are shown in Table S2.

Western blot
IL-1β, IL-6, TNF-α, IFN-γ and IL-10 in colonic tissue in each group were determined. After the colon tissue was ground into powder by liquid nitrogen, it was added into ice cold analysis buffer containing a cocktail of protection inhibitors. The mixture was lysed on ice for 30 min (mixed by repeated shaking with a vortex during this time to ensure complete cell lysis), and then the supernatant fluid of the lysate was collected (4℃, 12,000 rpm, 10 min). After electrophoresis, the proteins were electrotransferred onto a polyvinylidene fluoride (PVDF) membrane (Millipore, Boston, MA, USA). Then, the membrane was rinsed with blocking solution containing 5% skimmed milk for 2 h at room temperature and incubated with primary antibody overnight at 4℃. After the membranes were incubated with secondary antibody for 1 h at room temperature, the proteins were visualized using an enhanced chemiluminescence (ECL) system (Thermo Scientific, USA) and analyzed with ImageJ software. Antibodies are listed in Supplementary materials.

Immunohistochemistry
After the dewaxing of paraffin sections, the antigens were repaired by microwave heating and endogenous peroxidase was blocked by 3% hydrogen peroxide solution. The colon tissue sections were sealed at room temperature for 30 min with 3% BSA, and incubated at 4℃ overnight with rabbit anti-Foxp3 (A12051, ABclonal, Wuhan, PRC, 1:100 dilution). After that, the colon tissue sections were washed three times and incubated with goat anti-rabbit IgG (K5007, Dako, Shanghai, PRC, 1:200 dilution) at room temperature for 50 min. Sections of negative control were treated in the same manner, but the primary antibody was omitted. Three 400 visual fields were randomly selected for each slice in each group. ImageJ software was used to analyze each image to obtain the positive integrated optical density value (IOD) and the area of visual fields for each image, and then, calculate the mean optical density (MOD).

$$MOD = IOD/area$$

Colon contents untargeted metabolomic analysis
Metabolite extraction and UHPLC-MS/MS analyses were performed according to previous protocols (Want et al. 2013). The raw data files were processed using the Compound Discoverer 3.1 (CD 3.1, ThermoFisher, USA). After that, these metabolites were annotated using the KEGG, HMDB and LIPIDMaps database. Data normalization, partial least squares discriminant Aanalysis (PLS-DA), orthogonal partial least squares discriminant analysis (OPLS-DA) were performed with R package MetaboAnalystR (Chong and Xia 2018). To make the data close to a normal distribution, the Normalization function in the MetaboAnalystR package (with arguments MedianNorm, LogNorm, and AutoNorm) was adopted. We applied a univariate analysis (*t* test) to calculate the statistical significance (*p* value). The metabolites with VIP > 1, $p < 0.05$ and | log2 (fold Change) | > 1 were considered to be differential metabolites. The metabolites with $p < 0.05$ (*t* test) were used to conduct an over representation analysis (ORA), and the resulting KEGG pathways with $p < 0.05$ (ORA) were considered as statistically significant enrichment.

Qin *et al. Animal Diseases*   (2023) 3:16

Page 16 of 18

Data analysis

The normality of the data was tested using the Shapiro-Wilk normality test. The data that conformed to a normal distribution were analyzed by one-way ANOVA or t tests using the Graphpad Prism 6.0 software (GraphPad, La Jolla, CA, USA) and were presented as means±standard deviation (mean±SD). In addition, differential analysis of alpha diversity was performed using Wilcoxon rank sum test, beta diversity index was performed using the analysis of similarities (ANOSIM), and microbiota between different groups was performed using LEfSe. The significance level declared at ns $p > 0.05$, *$p < 0.05$, **$p < 0.01$ and ***$p < 0.001$.

Abbreviations

IBD	inflammatory bowel disease
UC	ulcerative colitis
AEA-P	arachidonoyl ethanolamide phosphate
CD	Crohn's disease
PCoA	principal coordinate analysis
LEfSe	Linear discriminant analysis Effect Size
DAI	disease activity index
MPO	myeloperoxidase
SOD	superoxide dismutase
MDA	malonaldehyde
IOD	integrated optical density
MOD	mean optical density
IL-1β	Interleukin-1 beta
IL-6	Interleukin-6
IL-10	Interleukin-10
TNF-α	Tumor necrosis factor- alpha
IFN-γ	Interferon Gamma
FOXP3	Forkhead box protein 3

Supplementary Information

The online version contains supplementary material available at https://doi.org/10.1186/s44149-023-00073-z.

Additional file 1: Fig. S1. Lincomycin had little destructive effect on small gut microbiota in mice. **Table S1.** Scoring system for Disease Activity Index (DAI). **Table S2.** Primers for RT-qPCR. **Table S3.** ANOSIM analysis of differential gut contents of Beta diversity (R > 0 means that the difference between groups is greater than that within groups, **$p < 0.01$, $^{ns}p > 0.05$). **Table S4.** ANOSIM analysis of Beta diversity between the DSS group and LP_DSS group (R>0 means that the difference between groups is greater than that within groups, **$p < 0.01$). Chemically-induced colitis/colon tumor mouse models.

Availability of data and materials

The materials and data not presented in this manuscript are available from the corresponding author upon request. The datasets generated during the current study are available in the NCBI repository, [https://www.ncbi.nlm.nih.gov/, PRJNA841483].

Declarations

Ethics approval and consent to participate
This study was approved by the Ethics Committee of Huazhong Agricultural U-niversity (Wuhan, China) (Permit No. HZAUMO-2021-0068 and HZAUMO-2021-0138) and performed based on the state guidelines from the Laboratory Animal Research Center of Hubei province in China.

Consent for publication
Not applicable.

Competing interests
The authors declare that they have no competing interests.

References

Adriaenssens, N., S. Coenen, A. Versporten, A. Muller, V. Vankerckhoven, H. Goossens, and ESAC Project Group. 2011. European surveillance of antimicrobial consumption (ESAC): quality appraisal of antibiotic use in Europe. *The Journal of Antimicrobial Chemotherapy.* 66: vi71–vi77. https://doi.org/10.1093/jac/dkr459.

Allen, I.C., J.E. Wilson, M. Schneider, J.D. Lich, R.A. Roberts, J.C. Arthur, R.M. Woodford, B.K. Davis, J.M. Uronis, H.H. Herfarth, C. Jobin, A.B. Rogers, and J.P. Ting. 2012. NLRP12 suppresses colon inflammation and tumorigenesis through the negative regulation of noncanonical NF-κB signaling. *Immunity.* 36 (5): 742–754. https://doi.org/10.1016/j.immuni.2012.03.012.

Arrieta, M.C., L.T. Stiemsma, P.A. Dimitriu, L. Thorson, S. Russell, S. Yurist-Doutsch, B. Kuzeljevic, M.J. Gold, H.M. Britton, D.L. Lefebvre, . 2015. Early infancy microbial and metabolic alterations affect risk of childhood asthma. *Science Translational Medicine* 7 (307): 307ra152. https://doi.org/10.1126/scitranslmed.aab2271.

Bárcena, C., R. Valdés-Mas, P. Mayoral, C. Garabaya, S. Durand, F. Rodríguez, M.T. Fernández-García, N. Salazar, A.M. Nogacka, N. Garatachea et al . 2019. Healthspan and lifespan extension by fecal microb-iota transplantation into progeroid mice. *Nature Medicine* 25 (8): 1234–1242. https://doi.org/10.1038/s41591-019-0504-5.

Bastaki, S.M., E. Adeghate, N. Amir, S. Ojha, and M. Oz. 2018. Menthol inhibits oxidative stress and inflammation in acetic acid-induced colitis in rat colonic mucosa. *American Journal of Translational Research* 10 (12): 4210–4222.

Bhinder, G., H.P. Sham, J.M. Chan, V. Morampudi, K. Jacobson, and B.A. Vallance. 2013. The *Citrobacter rodentium* mouse model: studying pathogen and host contributions to infectious colitis. *Journal of Visualized Experiments. JoVE* 72: e50222. https://doi.org/10.3791/50222.

Biagioli, M., A. Carino, C. Di Giorgio, S. Marchianò, M. Bordoni, R. Roselli, E. Distrutti, and S. Fiorucci. 2020. Discovery of a novel multi-strains probiotic formulation with improved efficacy toward intestinal inflammation. *Nutrients.* 12 (7): 1945. https://doi.org/10.3390/nu12071945.

Bokulich, N.A., B.D. Kaehler, J.R. Rideout, M. Dillon, E. Bolyen, R. Knight, G.A. Huttley, and J. Gregory Caporaso. 2018. Optimizing taxonomic classification of marker-gene amplicon sequences with QIIME 2's q2-feature-classifier plugin. *Microbiome.* 6 (1): 90. https://doi.org/10.1186/s40168-018-0470-z.

Callahan, B.J., P.J. McMurdie, M.J. Rosen, A.W. Han, A.J. Johnson, and S.P. Holmes. 2016. DADA2: High-resolution sample inference from Illumina amplicon data. *Nature Methods* 13 (7): 581–583. https://doi.org/10.1038/nmeth.3869.

Chong, J., and J. Xia. 2018. MetaboAnalystR: an R package for flexible and reproducible analysis of metabolomics data. *Bioinformatics (Oxford, England).* 34 (24): 4313–4314. https://doi.org/10.1093/bioinformatics/bty528.

Depommier, C., A. Everard, C. Druart, H. Plovier, M. Van Hul, S. Vieira-Silva, G. Falony, J. Raes, D. Maiter, N.M. Delzenne et al. 2019. Supplementation with

Qin *et al. Animal Diseases*   (2023) 3:16

Page 17 of 18

Akkermansia muciniphila in overweight and obese human volunteers: a proof-of-concept exploratory study. *Nature Medicine* 25 (7): 1096–1103. https://doi.org/10.1038/s41591-019-0495-2.

Dill-McFarland, K.A., P.J. Weimer, J.D. Breaker, and G. Suen. 2019. Diet influences early microbiota development in dairy calves without long-term impacts on milk production. *Applied and Environmental Microbiology* 85 (2): e02141–e02118. https://doi.org/10.1128/AEM.02141-18.

El Sayed, N.S., and A.S. Sayed. 2019. Protective effect of methylene blue on TNBS-induced colitis in rats mediated through the modulation of inflammatory and apoptotic signalling pathways. *Archives of Toxicology* 93 (10): 2927–2942. https://doi.org/10.1007/s00204-019-02548-w.

Fan, H., W. Chen, J. Zhu, J. Zhang, and S. Peng. 2019. Toosendanin alleviates dextran sulfate sodium-induced colitis by inhibiting M1 macrophage polarizati-on and regulating NLRP3 inflammasome and Nrf2/HO-1 signaling. *International Immunopharmacology* 76: 105909. https://doi.org/10.1016/j.intimp.2019.105909.

Geddes, A.M., R.A. Sleet, and J.M. Murdoch. 1964. Lincomycin hydrochloride: clinical and laboratory studies. *British Medical Journal* 2 (5410): 670–672. https://doi.org/10.1136/bmj.2.5410.670.

Glassner, K.L., B.P. Abraham, and E.M.M. Quigley. 2020. The microbiome and inflammatory bowel disease. *The Journal of Allergy and Clinical Immunology*. 145 (1): 16–27. https://doi.org/10.1016/j.jaci.2019.11.003.

Guo, Q., J.Z. Goldenberg, C. Humphrey, R. El Dib, and B.C. Johnston. 2019. Probiotics for the prevention of pediatric antibiotic-associated diarrhea. *The Co-chrane Database of Systematic Reviews*. 4 (4): CD004827. https://doi.org/10.1002/14651858.CD004827.pub5.

He, Y., C. Mao, H. Wen, Z. Chen, T. Lai, L. Li, W. Lu, and H. Wu. 2017. Influence of ad libitum feeding of piglets with bacillus subtilis fermented liquid feed on gut flora, luminal contents and health. *Scientific Reports* 7: 44553. https://doi.org/10.1038/srep44553.

Hviid, A., H. Svanström, and M. Frisch. 2011. Antibiotic use and inflammatory bo-wel diseases in childhood. *Gut*. 60 (1): 49–54. https://doi.org/10.1136/gut.2010.219683.

Imhann, F., A. Vich Vila, M.J. Bonder, J. Fu, D. Gevers, M.C. Visschedijk, L.M. Spekhorst, R. Alberts, L. Franke, H.M. van Dullemen et al. 2018. Interplay of host genetics and gut microbiota underlying the onset and clinical presentation of inflammatory bowel disease. *Gut*. 67 (1): 108–119. https://doi.org/10.1136/gutjnl-2016-312135.

Jia, J., K. Zheng, H. Shen, J. Yu, P. Zhu, S. Yan, Y. Xu, L. Zhu, Y. Lu, P. Gu, and W. Feng. 2020. Qingchang Huashi granule ameliorates experimental colitis via restoring the dendritic cell-mediated Th17/Treg balance. *BMC complementary medicine and therapies*. 20 (1): 291. https://doi.org/10.1186/s12906-020-03088-y.

Kaiko, G.E., S.H. Ryu, O.I. Koues, P.L. Collins, L. Solnica-Krezel, E.J. Pearce, E.L. Pearce, E.M. Oltz, and T.S. Stappenbeck. 2016. The colonic crypt protects stem cells from microbiota-derived metabolites. *Cell*. 165 (7): 1708–1720. https://doi.org/10.1016/j.cell.2016.05.018.

Kim, J.S., S.W. Kang, J.H. Lee, S.H. Park, and J.S. Lee. 2022. The evolution and competitive strategies of Akkermansia muciniphila in gut. *Gut Microbes* 14 (1): 2025017. https://doi.org/10.1080/19490976.2021.2025017.

Kronman, M.P., T.E. Zaoutis, K. Haynes, R. Feng, and S.E. Coffin. 2012. Antibiotic exposure and IBD development among children: a population-based cohort study. *Pediatrics*. 130 (4): e794–e803. https://doi.org/10.1542/peds.2011-3886.

Leppkes, M., and M.F. Neurath. 2020. Cytokines in inflammatory bowel diseases - Update 2020. *Pharmacological Research* 158: 104835. https://doi.org/10.1016/j.phrs.2020.104835.

Li, S., Y. Qi, L. Chen, D. Qu, Z. Li, K. Gao, J. Chen, and Y. Sun. 2019. Effects of Panax ginseng polysaccharides on the gut microbiota in mice with antibiotic-associated diarrhea. *International Journal of Biological Macromolecules* 124: 931–937. https://doi.org/10.1016/j.ijbiomac.2018.11.271.

Li, A., B. Liu, F. Li, Y. He, L. Wang, M. Fakhar-E-Alam Kulyar, H. Li, Y. Fu, H. Zhu, Y. Wang, and X. Jiang. 2021a. Integrated bacterial and fungal diversity analysis reveals the gut microbial alterations in diarrheic giraffes. *Frontiers in Microbiology* 12: 712092. https://doi.org/10.3389/fmicb.

Li, A., Y. Wang, Y. Wang, H. Dong, Q. Wu, K. Mehmood, Z. Chang, Y. Chang, L. Shi, Z. Tang, and H. Zhang. 2021b. Microbiome analysis reveals soil microbial commu-nity alteration with the effect of animal excretion contamination and altitude- in Tibetan Plateau of China. *International Soil and Water Conservation Res-earch*. 9 (4): 639–648. https://doi.org/10.1016/j.iswcr.

Li, Q., Y. Cui, B. Xu, Y. Wang, F. Lv, Z. Li, H. Li, X. Chen, X. Peng, Y. Chen, E. Wu, D. Qu, Y. Jian, and H. Si. 2021c. Main active components of Jiawei Gegen Qinlian decoction protects against ulcerative colitis under different dietary environments in a gut microbiota-dependent manner. *Pharmacological Research* 170: 105694. https://doi.org/10.1016/j.phrs.2021.105694.

Li, A., Y. Wang, M.F. Kulyar, M. Iqbal, R. Lai, H. Zhu, and K. Li. 2023. Environmental microplastics exposure decreases antioxidant ability, perturbs gut microbial homeostasis and metabolism in chicken. *The Science of the Total Environment*. 856 (1): 159089. https://doi.org/10.1016/j.scitotenv.

Liu, Y.J., B. Tang, F.C. Wang, L. Tang, Y.Y. Lei, Y. Luo, S.J. Huang, M. Yang, L.Y. Wu, W. Wang, S. Liu, S.M. Yang, and X.Y. Zhao. 2020. P-arthenolide ameliorates colon inflammation through regulating Treg/Th17 balanc-e in a gut microbiota-dependent manner. *Theranostics*. 10 (12): 5225–5241. https://doi.org/10.7150/thno.43716.

Liu, X., B. Mao, J. Gu, J. Wu, S. Cui, G. Wang, J. Zhao, H. Zhang, and W. Chen. 2021. Blautia-a new functional genus with potential probiotic properties? *Gut Microbes* 13 (1): 1–21. https://doi.org/10.1080/19490976.2021.1875796.

Lv, W., C. Liu, C. Ye, J. Sun, X. Tan, C. Zhang, Q. Qu, D. Shi, and S. Guo. 2017. Structural modulation of gut microbiota during alleviation of antibioti-c-associated diarrhea with herbal formula. *International Journal of Biological Macromolecules*. 105 (Pt3): 1622–1629. https://doi.org/10.1016/j.ijbiomac.2017.02.060.

Ma, C., S. Wasti, S. Huang, Z. Zhang, R. Mishra, S. Jiang, Z. You, Y. Wu, H. Chang, Y. Wang, D. Huo, C. Li, Z. Sun, Z. Sun, and J. Zhang. 2020. The gut microbiome stability is altered by probiotic ingestion and improved by the continuous supplementation of galactooligosaccharide. *Gut Microbes* 12 (1): 1785252. https://doi.org/10.1080/19490976.2020.1785252.

Maccarrone, M., T. Lorenzon, M. Bari, G. Melino, and A. Finazzi-Agro. 2000. Anandamide induces apoptosis in human cells via vanilloid receptors. Evidence for a protective role of cannabinoid receptors. *The Journal of biological chemistry*. 275 (41): 31938–31945. https://doi.org/10.1074/jbc.M005722200.

Macia, L., J. Tan, A.T. Vieira, K. Leach, D. Stanley, S. Luong, M. Maruya, C. I-an McKenzie, A. Hijikata, C. Wong et al. 2015. Metabolite-sensing rece-ptors GPR43 and GPR109A facilitate dietary fibre-induced gut homeostasis t-hrough regulation of the inflammasome. *Nature Communications* 6: 6734. https://doi.org/10.1038/ncomms7734.

Medzhitov, R. 2008. Origin and physiological roles of inflammation. *Nature*. 454 (7203): 428–435. https://doi.org/10.1038/nature07201.

Meira, L.B., J.M. Bugni, S.L. Green, C.W. Lee, B. Pang, D. Borenshtein, B.H. Rickman, A.B. Rogers, C.A. Moroski-Erkul, J.L. McFaline et al. 2008. DNA damage induced by chronic inflammation contributes to colon carcinogenesis in mice. *The Journal of Clinical Investigation*. 118 (7): 2516–2525. https://doi.org/10.1172/JCI35073.

Nguyen, L.H., A.K. Örtqvist, Y. Cao, T.G. Simon, B. Roelstraete, M. Song, A.D. Joshi, K. Staller, A.T. Chan, H. Khalili et al. 2020. Antibiotic use and the development of inflammatory bowel disease: a national case-control study in Sweden. *The Lancet. Gastroenterology & Hepatology*. 5 (11): 986–995. https://doi.org/10.1016/S2468-1253(20)30267-3.

Oka, A., and R.B. Sartor. 2020. Microbial-based and microbial-targeted therapies for inflammatory bowel diseases. *Digestive Diseases and Sciences* 65 (3): 757–788. https://doi.org/10.1007/s10620-020-06090-z.

Ozato, N., S. Saito, T. Yamaguchi, M. Katashima, I. Tokuda, K. Sawada, Y. Katsuragi, M. Kakuta, S. Imoto, K. Ihara, and S. Nakaji. 2019. Blautia genus associated with visceral fat accumulation in adults 20-76 years of age. *NPJ Biofilms and Microbiomes*. 5 (1): 28. https://doi.org/10.1038/s41522-019-0101-x.

Ozkul, C., V.E. Ruiz, T. Battaglia, J. Xu, C. Roubaud-Baudron, K. Cadwell, G.I. Perez-Perez, and M.J. Blaser. 2020. A single early-in-life antibiotic course increases susceptibility to DSS-induced colitis. *Genome Medicine* 12 (1): 65. https://doi.org/10.1186/s13073-020-00764-z.

Pittayanon, R., J.T. Lau, G.I. Leontiadis, F. Tse, Y. Yuan, M. Surette, and P. Moayyedi. 2020. Differences in gut microbiota in patients with vs without inflammatory bowel diseases: a systematic review. *Gastroenterology*. 158 (4): 930–946.e1. https://doi.org/10.1053/j.gastro.2019.11.294.

Qin, S., Z. Huang, Y. Wang, L. Pei, and Y. Shen. 2022. Probiotic potential of *Lactobacillus* isolated from horses and its therapeutic effect on DSS-induced c-olitis in mice. *Microbial Pathogenesis* 165: 105216. https://doi.org/10.1016/j.micpath.2021.105216.

Rol, Á., T. Todorovski, P. Martin-Malpartida, A. Escolà, E. Gonzalez-Rey, E. Aragón, X. Verdaguer, M. Vallès-Miret, J. Farrera-Sinfreu, E. Puig et al. 2021. Structure-based design of a Cortistatin analogue with immunomodulatory

Qin *et al. Animal Diseases*   (2023) 3:16

Page 18 of 18

activity in models of inflammatory bowel disease. *Nature Communications* 12 (1): 1869. https://doi.org/10.1038/s41467-021-22076-5.

Round, J.L., and S.K. Mazmanian. 2009. The gut microbiota shapes intestinal immune responses during health and disease. *Nature Reviews. Immunology* 9 (5): 313–323. https://doi.org/10.1038/nri2515.

Segata, N., J. Izard, L. Waldron, D. Gevers, L. Miropolsky, W.S. Garrett, and C. Huttenhower. 2011. Metagenomic biomarker discovery and explanation. *Genome Biology* 12 (6): R60. https://doi.org/10.1186/gb-2011-12-6-r60.

Singh, S. 2018. Evolution of clinical trials in inflammatory bowel diseases. *Current Gastroenterology Reports* 20 (9): 41. https://doi.org/10.1007/s11894-018-0648-3.

Song, M.Y., B.S. Kim, and H. Kim. 2014. Influence of Panax ginseng on obesity and gut microbiota in obese middle-aged Korean women. *Journal of Ginseng Research* 38 (2): 106–115. https://doi.org/10.1016/j.jgr.2013.12.004.

Vaz, L.E., K.P. Kleinman, M.A. Raebel, J.D. Nordin, M.D. Lakoma, M.M. Dutta-Linn, and J.A. Finkelstein. 2014. Recent trends in outpatient antibiotic use in children. *Pediatrics.* 133 (3): 375–385. https://doi.org/10.1542/peds.2013-2903.

Vázquez-Baeza, Y., M. Pirrung, A. Gonzalez, and R. Knight. 2013. EMPeror: a tool for visualizing high-throughput microbial community data. *GigaScience.* 2 (1): 16. https://doi.org/10.1186/2047-217X-2-16.

Vlahakos, D., N. Arkadopoulos, G. Kostopanagiotou, S. Siasiakou, L. Kaklamanis, D. Degiannis, M. Demonakou, and V. Smyrniotis. 2012. Deferoxamine attenuates lipid peroxidation, blocks interleukin-6 production, ameliorates sepsi-s inflammatory response syndrome, and confers renoprotection after acute he-patic ischemia in pigs. *Artificial Organs* 36 (4): 400–408. https://doi.org/10.1111/j.1525-1594.2011.01385.x.

Wang, H., C. Zhou, J. Huang, X. Kuai, and X. Shao. 2020. The potential therapeutic role of *Lactobacillus reuteri* for treatment of inflammatory bowel disease. *American Journal of Translational Research* 12 (5): 1569–1583.

Want, E.J., P. Masson, F. Michopoulos, I.D. Wilson, G. Theodoridis, R.S. Plumb, J. Shockcor, N. Loftus, E. Holmes, and J.K. Nicholson. 2013. Global metabolic profiling of animal and human tissues via UPLC-MS. *Nature Protocols* 8 (1): 17–32. https://doi.org/10.1038/nprot.2012.135.

Wu, J., Z. Wei, P. Cheng, C. Qian, F. Xu, Y. Yang, A. Wang, W. Chen, Z. Sun, and Y. Lu. 2020. Rhein modulates host purine metabolism in intestine thr-ough gut microbiota and ameliorates experimental colitis. *Theranostics.* 10 (23): 10665–10679. https://doi.org/10.7150/thno.43528.

Yamamoto, Y., J. Carreras, T. Shimizu, M. Kakizaki, Y.Y. Kikuti, G. Roncador, N. Nakamura, and A. Kotani. 2022. Anti-HBV drug entecavir ameliorates DSS-induced colitis through PD-L1 induction. *Pharmacological Research* 179: 105918. https://doi.org/10.1016/j.phrs.2021.105918.

Yu, P., C. Ke, J. Guo, X. Zhang, and B. Li. 2020. *Lactobacillus plantarum* L15 alleviates colitis by inhibiting LPS-mediated NF-κB activation and ameliorates DSS-Induced gut microbiota dysbiosis. *Frontiers in Immunology* 11: 575173. https://doi.org/10.3389/fimmu.2020.575173.

Zhang, Z., P. Shen, J. Liu, C. Gu, X. Lu, Y. Li, Y. Cao, B. Liu, Y. Fu, and N. Zhang. 2017. In vivo study of the efficacy of the essential oil of zanthoxylum bungeanum pericarp in dextran sulfate sodium-induced murine experimental colitis. *Journal of Agricultural and Food Chemistry* 65 (16): 3311–3319. https://doi.org/10.1021/acs.jafc.7b01323.

Zhou, Y., Z.Z. Xu, Y. He, Y. Yang, L. Liu, Q. Lin, Y. Nie, M. Li, F. Zhi, S. Liu et al. 2018. Gut microbiota offers universal biomarkers across ethnicity in inflammatory bowel disease diagnosis and infliximab response prediction. *mSystems* 3 (1): e00188–e00117. https://doi.org/10.1128/mSystems.00188-17.

Zhou, B.G., F.C. Liu, H.M. Zhao, X.Y. Zhang, H.Y. Wang, and D.Y. Liu. 2020. Regulatory effect of Zuojin Pill on correlation with gut microbiota an-d Treg cells in DSS-induced colitis. *Journal of Ethnopharmacology* 262: 113211. https://doi.org/10.1016/j.jep.2020.113211.